Concept of Assessing Nanoparticle Hazards Considering Nanoparticle Dosemetric and Chemical/Biological Response Metrics

Erik K. Rushton [a] , Jingkun Jiang [b] , Stephen S. Leonard [c] , Shirley Eberly [d] , Vincent Castranova [c] , Pratim Biswas [b] , Alison Elder [a] , Xianglu Han [a] , Robert Gelein [a] , Jacob Finkelstein [a e] & Günter Oberdörster [a]

[a] University of Rochester, Department of Environmental Medicine , Rochester, New York

[b] Washington University in St. Louis, Department of Energy, Environmental and Chemical Engineering , St. Louis, Missouri

[c] Pathology and Physiology Research Branch, Health Effects Laboratory Division , National Institute for Occupational Safety and Health , Morgantown, West Virginia

[d] University of Rochester, Dept. of Biostatistics and Computational Biology , Rochester, New York

[e] University of Rochester, Department of Pediatrics & Radiation Oncology , Rochester, New York, USA
Published online: 12 Feb 2010.

PLEASE SCROLL DOWN FOR ARTICLE

Taylor & Francis
Taylor & Francis Group

CONCEPT OF ASSESSING NANOPARTICLE HAZARDS CONSIDERING NANOPARTICLE DOSEMETRIC AND CHEMICAL/BIOLOGICAL RESPONSE METRICS

Erik K. Rushton[1], Jingkun Jiang[2], Stephen S. Leonard[3], Shirley Eberly[4], Vincent Castranova[3], Pratim Biswas[2], Alison Elder[1], Xianglu Han[1], Robert Gelein[1], Jacob Finkelstein[1,5], Günter Oberdörster[1]

[1]University of Rochester, Department of Environmental Medicine, Rochester, New York
[2]Washington University in St. Louis, Department of Energy, Environmental and Chemical Engineering, St. Louis, Missouri
[3]Pathology and Physiology Research Branch, Health Effects Laboratory Division, National Institute for Occupational Safety and Health, Morgantown, West Virginia
[4]University of Rochester, Dept. of Biostatistics and Computational Biology, Rochester, New York
[5]University of Rochester, Department of Pediatrics & Radiation Oncology, Rochester, New York, USA

Engineered nanoparticles (NP) are being developed and incorporated in a number of commercial products, raising the potential of human exposure during manufacture, use, and disposal. Although data concerning the potential toxicity of some NP have been reported, validated simple assays are lacking for predicting their *in vivo* toxicity. The aim of this study was to evaluate new response metrics based on chemical and biological activity of NP for screening assays that can be used to predict NP toxicity *in vivo*. Two cell-free and two cell-based assays were evaluated for their power in predicting *in vivo* toxicity of eight distinct particle types with widely differing physicochemical characteristics. The cell-free systems comprised fluorescence- and electron spin resonance-based assays of oxidant activity. The cell-based systems also used electron spin resonance (ESR) as well as luciferase reporter activity to rank the different particle types in comparison to benchmark particles of low and high activity. *In vivo* experiments evaluated acute pulmonary inflammatory responses in rats. Endpoints in all assays were related to oxidative stress and responses were expressed per unit NP surface area to compare the results of different assays. Results indicated that NP are capable of producing reactive species, which in biological systems lead to oxidative stress. Copper NP had the greatest activity in all assays, while TiO_2 and gold NP generally were the least reactive. Differences in the ranking of NP activity among the assays were found when comparisons were based on measured responses. However, expressing the chemical (cell-free) and biological (cells; *in vivo*) activity per unit particle surface area showed that all *in vitro* assays correlated significantly with *in vivo* results, with the cellular assays correlating the best. Data from this study indicate that it is possible to predict acute *in vivo* inflammatory potential of NP with cell-free and cellular assays by using NP surface area-based dose and response metrics, but that a cellular component is required to achieve a higher degree of predictive power.

Nanoparticles (NP) are in the same size range (<100 nm) as ambient ultrafine particles (UFP), and lessons learned from epidemiological, clinical, and animal studies with UFP indicate that inhalation exposure to these particles is associated with and results in significant adverse health effects (von Klot et al., 2005; Ibald-Mulli et al., 2002; Utell & Frampton, 2000; U.S. EPA, 2004; Oberdorster et al., 1994; Craig et al., 2008). Indeed, concerns about the safety of engineered NP were expressed by scientists, governmental, and nongovernmental organizations (The Royal Society, 2004; Environmental Defense, 2007; Oberdorster et al., 2005a; Maynard et al., 2006; Borm et al., 2006; U.S. EPA, 2007;). Some of the unique properties that make NP valuable for numerous industrial and biomedical applications are also likely to increase their hazardous potential, for example, an increased chemical reactivity due to a large surface area per volume. However, reports regarding potential adverse effects are limited to only a tiny fraction of NP including TiO_2, carbon nanotubes, buckyballs, and quantum dots. Most of these effects were observed in *in vitro* and some *in vivo* studies using excessively high doses so that direct extrapolation of these results to humans under realistic lower exposure scenarios has to be questioned. The rapid increase of newly engineered NP makes it impossible for ethical and economic reasons to assess their toxic potential using laboratory animal tests; thus, there is an urgent need to develop and validate simple high-throughput assays to determine nanoparticle toxicity (Brown et al., 2001; Dick et al., 2003; Oberdorster et al., 2005b; Nel et al., 2006; Balbus et al., 2007; Maynard, 2007).

An International Life Sciences Institute Nanomaterial Toxicity Screening Working Group suggested a tiered approach for assessing NP toxicity, including cell free, *in vitro* and *in vivo* assays (Oberdorster et al., 2005b). Since there were no agreed-upon standard tests, a list of endpoints based on effects of interest was presented, including oxidant production. Oxidative stress was proposed as a central mechanism by which NP might induce toxicity

(Brown et al., 2001; Nel et al., 2006). It was postulated that it is possible to identify a simple test that is predictive for the acute *in vivo* toxicity for NP with diverse physicochemical characteristics when it is based on the mechanism of oxidative stress induction. Specifically, the hypothesis was tested that a comparison of the prediction of *in vivo* responses from results of different assays not *in vivo* is best achieved when responses are expressed per unit of dose (preferably using particle surface area as the dose metric), as suggested in a recent publication by Jiang et al. (2008). Such a surface-area-based response-metric enables a comparison of assays at equivalent dose levels, thereby avoiding problems associated with irrelevant high doses.

Ideally, doses in this approach would be selected that are in the steepest section of a dose-response curve because this section reflects the maximum responses per unit dose. It was suggested that this represents the most appropriate point for comparing responses among different assays. An increase in dose beyond this steepest part results in a lower response per unit dose, possibly indicating saturation of biotransformation processes, binding sites, or defense mechanisms or a shift to a different physiological response pathway.

This response-metric concept was tested in a pilot-type proof-of-principle study by determining chemical (cell-free assays) and biological responses (cell and *in vivo* assays). The experiments described herein included eight NP with a broad range of different physicochemical properties. Their activities were evaluated using assay systems that centered on oxidant stress: (1) determination of the intrinsic reactive oxygen species (ROS)-generating potential of NP in two cell free systems; (2) induction of oxidative stress responses in a lung epithelial cell line and in macrophages; and (3) acute pulmonary inflammatory responses in rats following intratracheal administration of NP. Comparing results of different assays can be difficult because dose levels and dose rates vary greatly, for example, *in vitro* bolus delivery versus *in vivo* inhalation. Thus, for the purpose of this initial proof-of-principle

study, dosing was by bolus-type delivery of NP in all assays. With the exception of one cell-free assay, a full dose-response relationship was not established for each assay, but a single dose was selected that was judged as not excessively high.

In an additional test of the validity of our concept, this was applied to published results of a well-designed study by Sayes et al. (2007) with the objective of assessing the capacity of *in vitro* screening assays to predict *in vivo* pulmonary inflammation of several fine and nanoscale particles in rats. Sayes et al. (2007) found little correlation between *in vitro* cytotoxicity and *in vivo* inflammation. Because complete dose-response relationships were established in that study, it was not possible to determine the maximum response per unit dose (steepest section of dose-response) and test the response-metric concept.

METHODS

Nanoparticle Sources

Elemental carbon particles were generated in house via an electric spark discharge ultrafine particle generator (approximately 41 nm, PALAS, Germany). $TiO_2(F)$ (approximately 250 nm) was purchased from Fischer Scientific (Fairlawn, NJ). $TiO_2(M)$ (approximately 20 nm) was a gift from Millenium Chemical Corporation (Hunt Valley, MD). $TiO_2(D)$ (P25, approximately 25 nm) was a gift from Degussa Chemicals (Hanau, Germany). Copper (Cu) (40 nm) and Ag (35 nm; a silver NP interlaced with a carbon matrix referred to hereafter as silver NP), were gifts from Nanotechnologies, Inc. (Austin, TX). Au (50 nm) was purchased from Ted Pella (Redding, CA). Aminated polystyrene ($PS-NH_3$) (~60 nm) particles were purchased from Bangs Laboratories (Fishers, IN).

Physicochemical Characteristics of NP

The crystallinity of samples was characterized by X-ray diffraction using a Rigaku Geigerflex D-MAX/A diffractometer with Cu-Kα radiation. BET isotherms (Autosorb-1, Quantachrome) were used to measure the specific surface area of NP with nitrogen adsorption at 77 K. The BET equivalent particle diameter was calculated based upon the specific surface area and the particle density. The agglomerate state and surface charge of NP in solution were characterized with a ZetaSizer Nano ZS (Malvern Instruments, Inc., Malvern, PA) utilizing dynamic light scattering and electrophoretic mobility, respectively. The mean hydrodynamic diameter and zeta potential of each sample in distilled deionized water are reported. All NP preparations were endotoxin free, as determined by a *Limulus* amebocyte lysate (LAL) assay (Lonza, Walkinsville, MD).

Reagents Used in Cell-Free and Cellular Assays

2',7'– Dichlorofluorescein diacetate (DCF-DA) was purchased from Calbiochem, (San Diego, CA). Sodium phosphate was from J. T. Baker (Phillipsburg, NJ). Lyophilized horseradish peroxidase was purchased from Pierce Chemical Company (Rockford, IL). Hydrogen peroxide (H_2O_2) and 5,5-dimethyl-l-pyrroline *N*-oxide (DMPO) were purchased from Sigma (St. Louis, MO). Phosphate-buffered saline (PBS) and RPMI-1640 medium were purchased from Gibco BRL (Gaithersburg, MD). The spin trap DMPO was purified by charcoal decolorization and vacuum distillation. DMPO solution, thus purified, did not contain any electron spin resonance (ESR)-detectable impurities. Chelex 100 chelating resin was purchased from Bio-Rad Laboratories (Richmond, CA). The phosphate buffer (pH 7.4) was treated with Chelex 100 to remove transition metal ion contaminants. Hanks balanced salt solution (HBSS) was purchased from Mediatech (Herndon, VA). Defined fetal bovine serum (FBS) was purchased from Hyclone (Logan, UT). Luciferase Assay System was purchased from Promega Corporation (Madison, WI).

Cell-Free ROS Generation

The goal of this assay was to measure the intrinsic radical electron inducing capacity of NP in phosphate buffer utilizing DCFH-DA, which detects ROS and reactive nitrogen species (RNS) and is, thus, broad in its specificity. This assay is modified from Venkatachari et al. (2005) and was performed as follows: Deacetylated

non-fluorescent dye is oxidized to its fluorescent form by radical electrons that are transferred from the NP surface via HRP. Results are expressed as hydrogen peroxide (H_2O_2) equivalents based on a standard curve (0, 1, 2, 5, 10, 20, and 40 μM H_2O_2).

DCFH-DA was reconstituted in ethanol (5 mM) and stored at –20°C until use. Sodium phosphate buffer (25 mM) was prepared at pH 7.2. The dye was deacetylated by slightly modifying a procedure developed previously (Venkatachari et al., 2005; Cathcart et al., 1983). One part 5 mM DCF-DA was mixed with 40 parts 0.01 N sodium hydroxide for 30 min at room temperature in an opaque vessel, which facilitates cleavage of the diacetate group. Then 200 parts of sodium phosphate buffer was added to neutralize the reaction. The mixture was kept on ice until ready to use. Just prior to use, horseradish peroxidase (HRP) was added to serve as a catalyst (2.2 U/ml). The working concentration of DCF was 21 μM.

A stock suspension of NP (except PS and gold NP) was dispersed in sodium phosphate buffer via probe sonication (1000 J for 5 s). The PS and gold NP were vortexed in the suspensions received by the supplier and an aliquot added to the buffer and either water bath sonicated (PS) or vortexed (gold) to obtain the final concentrations for the assay. Nothing was added to the suspensions prior to, during, or after sonication to prevent agglomeration of the particles. From the stock suspension, increasing doses of particles (via increasing volumes) were added to 13 × 100 mm borosilicate glass tubes in triplicate. Sodium phosphate buffer was added to each tube to normalize the differences in volume. Control sodium phosphate buffer was also sonicated and used as a vehicle control. Dose-response (as H_2O_2 equivalents) relationships were created for each NP. Since the ROS-inducing potential of NP varied widely, different concentrations were used for each NP type in order to stay within the detection limits of the assay. Concentrations ranged from 0.08 to 0.33 µg/ml for Cu NP to 160 to 3300 µg/ml for polystyrene NP.

In a dark room, 3 ml of prepared dye was added to the standards (H_2O_2) and to the samples and incubated in a 37°C water bath for 15 min. At the end of incubation, the fluorescence was quantitated using a fluorometer (Turner TD 700) at an excitation wavelength of 486 nm and emission wavelengths from 570 to 700 nm. A straight-line fit was applied to the standards and the equation of the line was used to express the results of the particle measurements as H_2O_2 equivalents. All standards and samples were run in duplicate.

Higher concentrations of the suspended NP might potentially interfere with the fluorescence reading by quenching or altering light transmission. This was tested by taking fluorometer readings at the end of incubation in samples after eliminating the particles by centrifugation at 10,000 × g for 15 min and comparing these to the un-spun samples. All results are reported from the centrifuged samples; only higher concentrations of PS-NP interfered with the assay, while none of the other NP did.

Electron Spin Resonance Assay

Cell Free Assay Spin trapping was used to detect short-lived free radical intermediates. This technique involved the addition-type reaction of a short-lived radical with a paramagnetic compound (spin trap) to form a relatively long-lived free radical product (spin adduct), which was then studied using conventional ESR. The radical generation potential of the particles was examined by reacting them in a cell-free system with H_2O_2, which is found in cells and generates the hydroxyl radical upon reaction with transition metals through a Fenton-like reaction. This reaction is used to measure the reactivity potential of a material (Leonard et al., 2004; Masaki & Sakurai, 1997).

All ESR measurements were conducted using a Bruker EMX spectrometer (Bruker Instruments, Inc., Billerica, MA) and a flat cell assembly. The intensity of the signal was used to measure the amount of short-lived radicals trapped; the hyperfine couplings of the spin adduct were generally characteristic of the

original trapped radicals. Hyperfine couplings were measured (to 0.1 G) directly from magnetic field separation using potassium tetraperoxochromate (K_3CrO_8) and 1,1-diphenyl-2-picrylhydrazyl (DPPH) as reference standards. The relative radical concentration was estimated by multiplying half of the peak height by $[\Delta Hpp]^2$, where ΔHpp represents peak-to-peak width. An Acquisit program was used for data acquisition and analysis.

Reactants (H_2O_2, various particles (10 mg/ml), and 100 mM of the spin trap DMPO were mixed in a final volume of 1 ml suspended in PBS. The H_2O_2 was added to the system to serve as an exogenous surrogate source that would normally be produced by inflammatory cells. It serves as a ROS precursor upon which the particles act to produce hydroxyl radicals to be measured via ESR. The reaction mixture was then transferred to a flat cell, and ESR measurements were conducted after a 3-min incubation period. Experiments were performed at room temperature and under ambient air.

ESR Assay With Cells (AM)   Alveolar macrophages (AM, 10^6) were obtained from Sprague-Dawley rats (Castranova et al., 1990) and mixed with DMPO (200 mM) and particles (1 mg/ml) with PBS to a final volume of 1 ml. The mixtures were then incubated for 5 min in a 37°C water bath. The reaction mixture was then transferred to a flat cell for ESR measurement. The concentrations given in the figure legends are final concentrations. Experiments were performed at room temperature under ambient air.

Specific-pathogen-free male Sprague-Dawley (Hla: (SD) CVF) rats weighing 200–300 g obtained from Hilltop Lab Animals (Scottdale, PA) were used. The animals were housed in an AAALAC- International-accredited, specific-pathogen-free, environmentally controlled facility. Rats were acclimated for at least 5 d before use and were housed in ventilated cages that were provided HEPA-filtered air, with Alpha-Dri virgin cellulose chips and hardwood Beta Chips used as bedding. The rats were maintained on ProLaB 3500 diet and tap water, both of which were provided ad libitum. The rats were euthanized with an ip

injection of 100 mg sodium pentobarbital/kg body weight. Bronchoalveolar lavage (BAL) was conducted with Ca^{2+}/Mg^{2+}-free phosphate buffered saline (PBS, pH 7.4) plus 5.5 mM D-glucose as described (DiMatteo et al., 1996; Porter et al., 2002). A tracheal cannula was inserted, and BAL was performed using ice-cold PBS. The first lavage was 6 ml; subsequent lavages used 8 ml of PBS until a total of 100 ml of lavage fluid was collected. The BAL cells were pelleted (650 × g, 10 min, 4°C), washed once, and resuspended in PBS. AM and polymorphonuclear leukocyte (PMN) cell counts were obtained using an electronic cell counter equipped with a cell sizer (Coulter Multisizer II, Coulter Electronics, Hialeah, FL), as previously described (Castranova et al., 1990).

Luciferase Reporter Activity in Lung Epithelial Cells

The goal of this assay was to measure ROS induction by activated cells utilizing an oxidant-sensitive luciferase reporter. A stable luciferase-transfected human type II lung epithelial cell line, A549 Luc1, was used to quantify NP induced ROS activity (Singal & Finkelstein, 2005). Cells were allowed to become synchronous via 24-h incubation in serum-free medium. At the end of serum deprivation, cells were exposed to 9.5 μg particles/cm^2 for 24 h in medium containing 1% FBS (Barrett et al., 1999).

A549 Luc1 cells were seeded in 12 well plates and grown in RPMI-1640 medium containing 10% FBS and 0.6 μL/ml gentamicin to 75% confluency. NP received as dry powders were probe sonicated as in cell-free investigations (5 s, 1000 J). Gold and PS NP received as suspensions were treated differently. A volume of gold NP of required mass was coated with proteins by incubating with an equivalent volume of FBS for 30 min. Following incubation, the particles were spun at 20,000 × g for 30 min. The FBS was aspirated and the remaining pellet was suspended in media with 1% FBS to make a 0.2-mg/ml stock suspension (the same as for the dry powders). For the PS particles the required volume was added to

media with 1% FBS to make a 0.2-mg/ml stock suspension. Following addition of the medium, particles were sonicated (5 s, 1000 J) and subsequently diluted for cellular assays. At the end of the incubation, cells were washed two times with PBS. Luciferase activity in adherent cell lysates was measured according to kit instructions. In brief, 120 μl of luciferase cell culture lysis reagent was added per well and rocked at room temperature for 30 min. The lysate was transferred to a microcentrifuge tube, vortexed, then centrifuged (12,000 × g, 2 min, 4°C). The supernatant was transferred to a microplate and luciferase (fluorescence) activity was read on a Spectramax M5 plate reader (Molecular Devices Corporation, Sunnyvale, CA).

In Vivo Inflammatory Responses to NP

Specific-pathogen-free male Fischer 344 rats (8 wk; 240 to 260 g) were obtained from Harlan (Indianapolis, IN). Rats were housed in plastic cages with Alpha-Dri bedding with wire tops and filtered bonnets in an AAALAC International-accredited facility and were allowed to acclimate for at least 1 wk prior to use in experimental protocols. All animals were given free access to Rodent Diet 5001 (LabDiet, St. Louis, MO) and water and were housed in an air-conditioned barrier facility with a 12-h light–dark cycle.

For intratracheal dosing, the rats were anesthetized with isoflurane (5%, Baxter Scientific, Deerfield, IL) and placed in a supine position at a 45° angle. A pediatric otoscope allowed for placement of a catheter (22-gauge iv catheter sheath attached to a 21-gauge blunted needle) between the vocal cords. The breathing cycles were monitored using a Respiband inductive coil wrapped around the lower rib cage and the signal was displayed on a Respigraph Series 4712 oscilloscope (NIMS, Miami Beach, FL), and particle suspensions were instilled into the lungs (250 μl) at the start of an inspiratory phase. Particles in powder form were used to prepare stock suspensions in sterile pyrogen-free saline (Abbot Laboratories, North Chicago, IL). Prior to instillation, stock suspensions were probe sonicated (5 s,

1000 J). Particles received in aqueous suspension were either vortexed (gold NP) or water bath sonicated (PS NP). The PS NP were added to pyrogen-free saline and vortexed prior to instillation. The gold NP were spun down and resuspended in pyrogen-free distilled water and vortexed prior to instillation. In separate studies it was determined that intratracheal instillation in rats of 250 μl distilled water, like physiological saline, did not induce a significant inflammatory response by 24 h.

In order to remain within the steep section of the inflammatory response, 25 μg of Cu NP was instilled, while 100 μg was used for the other NP. Twenty-four hours after exposure, rats were sacrificed with a lethal ip dose of sodium pentobarbital (0.1 mg/kg, Abbott Laboratories, North Chicago, IL) and exsanguinated via the abdominal aorta. Lungs were excised, weighed, and lavaged five times (5 ml of 0.9% pyrogen-free saline each time). The first two lavages were kept separate for biochemical analyses of the supernate (protein, lactate dehydrogenase [LDH], beta-glucuronidase). Lavage cells were spun down, combined, and a total cell count, cell type differential, and viability were evaluated.

Statistical Analysis

Data are represented as means ± SE. Statistically significant differences from controls in the *in vivo* and *in vitro* cellular (A549 Luc) assays were analyzed using Student's *t*-test. The level of significance was set at $p < .05$. Results of all five assays were initially correlated with the dose expressed as particle mass, number, or surface area; NP surface area was used as the dose metric for further analysis. Responses were then expressed as per unit of NP surface area as the response-metric chemical (cell-free assays) or biological (cellular, *in vivo* assays) (Jiang et al., 2008). Only then was it meaningful to compare results of the different assays with each other. For example, the cell-free ROS assay response (H_2O_2 equivalent μmol/cm^2 NP surface) was compared with the *in vivo* response (number of PMN/cm^2 NP surface), using the BET surface listed in Table l.

TABLE 1. Physicochemical Properties of Investigated Nanoparticles*

Particle	Origin	Primary particle size (nm) (a)	Crystal phase	Specific surface area (m²/gm) (BET)	BET equivalent diameter (nm)	Hydrodynamic diameter (nm) (b)	Zeta potential (mV) (c)	Sample aggregation degree
Elemental carbon (EC)	Electric spark generated (Rochester)	41	Amorphous	768	3.4	204	−50.5	High
TiO₂(F)	Fischer Scientific	250	Anatase	8	195	1287	−14.7	Medium
TiO₂(M)	Millenium Chemical Corp.	~20	Anatase	86	18.3	1608	14	High
TiO₂(D)	Degussa Chemicals	~25	80% anatase/ 20% rutile	57	27	576	27.3	Medium
Copper	Nanotechnologies	40	FCC crystal	31	21.9	850	−0.6	Medium
Silver	Nanotechnologies	35	FCC crystal	21	27.3	483	−47.0	Medium
Au	Ted Pella (Ca)	50	FCC crystal	6[d]	53[e]	93	−33.8	Low
PS-NH₃	Bangs Laboratories	65	Amorphous	88[d]	65[f]	72	83.0	Very low

Note. Particle sizes as provided by the manufacturer (in the case of electric spark generated carbon in our laboratory the count median diameter in the air) are listed, and all the other measurements were made in our own laboratories. The agglomeration state was estimated to range from very low to high based on the differences between BET equivalent diameter and hydrodynamic diameter and examination of TEM pictures. (a) Size as reported by manufacturer. (b) Measured by dynamic light scattering in water. (c) Measured by electrophoretic mobility in water. (d) Calculated based on primary particle size. (e) TEM measurements. (f) Based on manufacturer report.

Assay mean values were base 10 log-transformed, and linear regression techniques were used to evaluate the correlation between the *in vivo* responses and the results from the other assays.

RESULTS

NP Physicochemical Characteristics

The physicochemical characteristics of the eight NP are given in Table 1. With the exception of gold and polystyrene (PS) NP, all other NP were agglomerated in water; elemental carbon and 20 nm anatase appeared to be highly aggregated.

Cell-Free, Cell, and *In Vivo* Assays

Cell-Free ROS Assay The intrinsic capacity of the eight NP to induce ROS ranged from highly reactive Cu NP to low-activity TiO₂ and polystyrene NP. Figure 1A shows the results expressed as H_2O_2 equivalent activity/µg/NP. The concentrations required to elicit a response varied widely from 0.08 to 3300 µg/ml, dependent on NP chemical composition and crystallinity. Comparing the results of this assay on a mass or surface area basis resulted in

dose-response curves that are quite similar, although there is a greater separation between the different NP when the dose was expressed as surface area. For example, a notable difference between mass-based and surface-area-based ROS activity was the response to carbon NP relative to that of the other NP, which shifted from more reactive based on mass to less reactive based on surface area; gold NP and TiO₂-F became more reactive relative to the other NP when dose was based on surface area.

Electron Spin Resonance Analysis via Spin Trapping, Cell-Free Assay Results indicate that Cu NP generated significant levels of hydroxyl radicals in the presence of H_2O_2 (Figure 1B). The inset shows a typical ESR spectrum generated from a mixture containing particles plus H_2O_2 in the presence of DMPO as a spin trap. This spectrum consists of a 1:2:2:1 quartet with splitting of $a_H = a_N = 14.9$ G. Based on these splitting constants, the 1:2:2:1 quartet was assigned to a DMPO/·OH adduct. TiO₂ NPs exhibited significant but lower radical generation potential than Cu NP and quantitative differences in activity between the different TiO₂ NP may be due to different
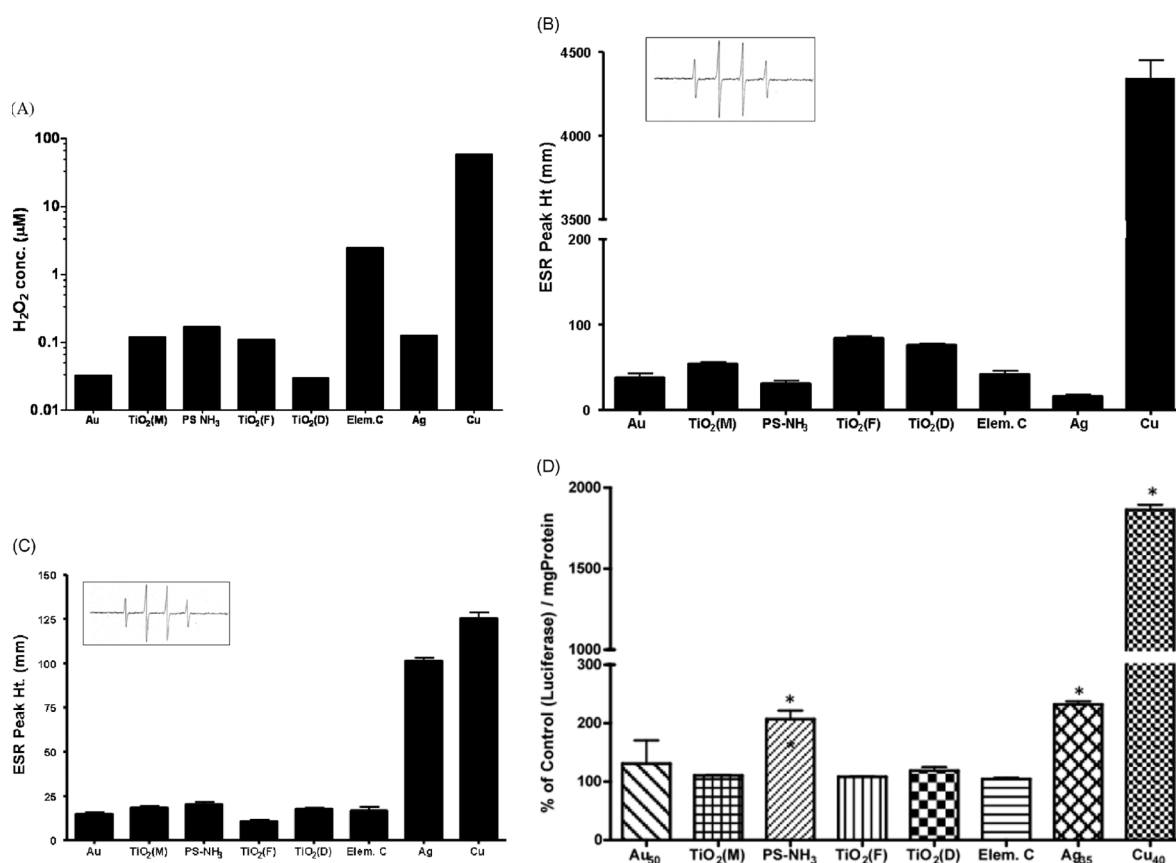
FIGURE 1. A: Cell-free ROS activity by different nanoparticles using DCF-DA fluorescence assay in a phosphate buffer. Data are expressed as H_2O_2 equivalent activity per μg of nanoparticles. B: Cell-free generation of hydroxyl radicals by different nanoparticles, determined by ESR. Results show ESR peak height (hydroxyl radical) for 10 mg/ml of each particle suspended in 1 ml PBS containing l mM H_2O_2 in the presence of DMPO. Inset shows a typical 1:2:2:1 hydroxyl radical spectrum. Bars represent average values (n = 3) ± standard error. C: Cellular generation of hydroxyl radical in the presence of different nanoparticles determined by ESR. Results shows ESR peak height for 1 mg/ml of each particle after 5 min. incubation with rat alveolar macrophages in PBS in the presence of DMPO. Inset shows a typical 1:2:2:1 hydroxyl radical spectrum from cells. Bars represent average values (n = 3) ± standard error. D: Luciferase production by A549 Luc-1 cells upon nanoparticle stimulation following 24-hr. incubation at 9.5 μg/cm^2. Bars represent average values (n = 3) ± standard error. *p < 0.05.

crystallinities. In general, the same concentration of the other particles did not exhibit substantial ESR signal, reflecting low hydroxyl radical-producing ability in the presence of H_2O_2.

Hydroxyl Radical Generation in the Presence of AM The possible generation of free radicals from the interaction of NPs with rat AM was also examined, using ESR spin trapping. Figure 1C shows ESR peak heights of the DMPO/·OH adduct produced by cells exposed to NP. As in the cell-free assays, the particles that demonstrated the most activity were the Cu NP. However, in contrast to the cell-free

ESR assay, Au NP demonstrated an ability to produce radicals in the presence of AM. The inset shows a typical. OH radical spectrum generated from cells reacting with particles.

In Vitro **Luciferase Production** Luciferase production following *in vitro* exposure of A549 cells was dependent on the NP type. Most NPs produced a minimal but detectable response in this screening assay. Aminated PS and Au NP produced a 2-fold rise in luciferase production, while Cu NP increased this production more than 15-fold, as shown in Figure 1D. All data have been normalized to total protein concentration.

***In Vivo* Inflammatory Response**   Figure 2 shows the number of polymorphonuclear leukocytes (PMN) in BAL fluid from rats 24 h after intratracheal instillation of 25 µg of Cu NP or 100 µg of the other NP. Copper elicited a high inflammatory response; cell differential analysis of cytospin preparations indicates that 61.8% of the BAL cells were PMN. In addition, increases in AM and lymphocytes as well as total cell numbers were also observed. The second most inflammatory particle was Au, followed by carbon. The gold NP produced the least inflammation of the particles tested. Among the titanium dioxides tested, the lavage PMN response varied with the type of titanium dioxide, with $TiO_2(D)$ having the highest inflammatory potential of this subset even though the response itself was mild in nature.

Detailed results of BAL cellular and biochemical analyses are listed in Table 2. Of note is the low percentage of PMN in the controls.

In Vitro—In Vivo Correlations

Figure 3 represents log–log plots of the NP surface-area-normalized PMN responses after *in vivo* exposures (ordinate) versus the NP surface-area-normalized responses of the other assays (abscissa).

Copper NP had the highest activity in each assay; however, ranking orders within the individual assays based on the administered mass dose were different and good correlations to *in vivo* responses were not obvious. In order to apply our concept of expressing responses per unit of the administered dose and selecting the particle surface area as the dose metric, the
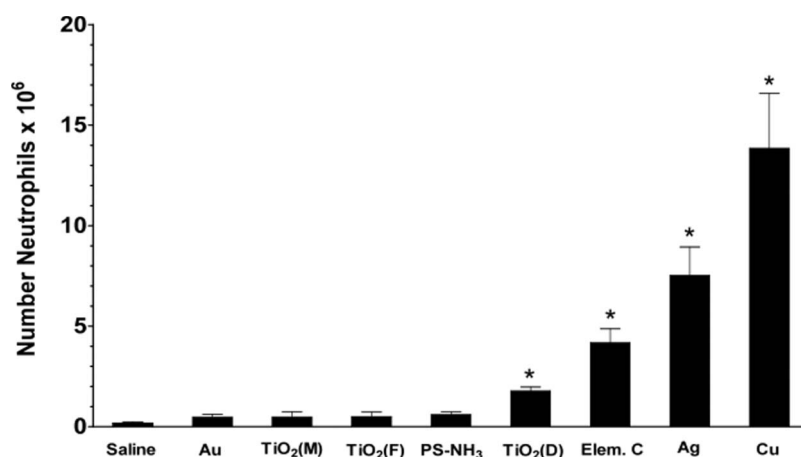

FIGURE 2. Pulmonary inflammatory response of nanoparticles determined by number of neutrophils (PMN) in lung lavage 24 hrs. after intratracheal instillation of 100 µg (25 µg for copper NPs) in rats. Bars represent average values (n = 3-5) ± standard error. *p < 0.05.

TABLE 2. *In Vivo* Bronchoalveolar Lavage Parameters of Rats 24 h After Intratracheal Instillation of 100 µg of Ns (25 µg Copper NP)

	Total cells × 10⁷	Percent macrophages	Percent PMN	Percent lymphocytes	Percent viable	Protein (mg/ml)	LDH (nmol/ml/min)	β-Glucuronidase (nmol/ml/min)
Saline	1.597 (0.190)	98.1 (0.4)	1.1 (0.5)	1.1 (0.6)	95.6 (1.1)	0.154 (0.007)	59.668 (9.232)	0.367 (0.060)
TiO₂(D)	1.488 (0.019)	86.7 (2.0)	12.0 (2.0)	1.4 (0.2)	96.2 (0.5)	0.122 (0.015)	67.574 (4.786)	0.142 (0.015)
TiO₂(F)	1.091 (0.143)	94.63 (2.4)	4.4 (2.7)	1.2 (0.4)	92.7 (1.0)	0.186 (0.008)	52.250 (2.461)	0.311 (0.006)
TiO₂(M)	1.473 (0.118)	95.4 (3.9)	3.3 (3.5)	1.3 (0.63)	96.1 (1.0)	0.116 (0.005)	60.895 (6.237)	0.311 (0.036)
Ag	2.269 (0.238)	65.2 (8.7)	33.8 (8.9)	1.0 (0.5)	97.1 (0.5)	0.237 (0.028)	105.233 (16.166)	0.998 (0.260)
Cu	2.706 (0.951)	47.5 (10.9)	50.8 (10.5)	1.8 (0.6)	95.3 (0.8)	0.696 (0.243)	191.592 (52.413)	2.861 (0.758)
Au	1.545 (0.332)	96.2 (2.2)	2.8 (1.6)	0.9 (0.6)	93.2 (2.7)	0.188 (0.010)	76.916 (8.462)	0.316 (0.010)
C	1.845 (0.288)	75.3 (7.5)	22.4 (6.1)	2.4 (2.1)	96.1 (0.4)	0.218 (0.024)	115.658 (8.274)	0.688 (0.086)
PS-NH₃	1.591 (0.167)	95.3 (2.0)	3.9 (1.8)	0.8 (0.4)	94.5 (1.6)	0.153 (0.009)	76.848 (7.668)	0.331 (0.057)

Note. Values represent the mean of three to five animals; standard deviations are shown in parentheses.
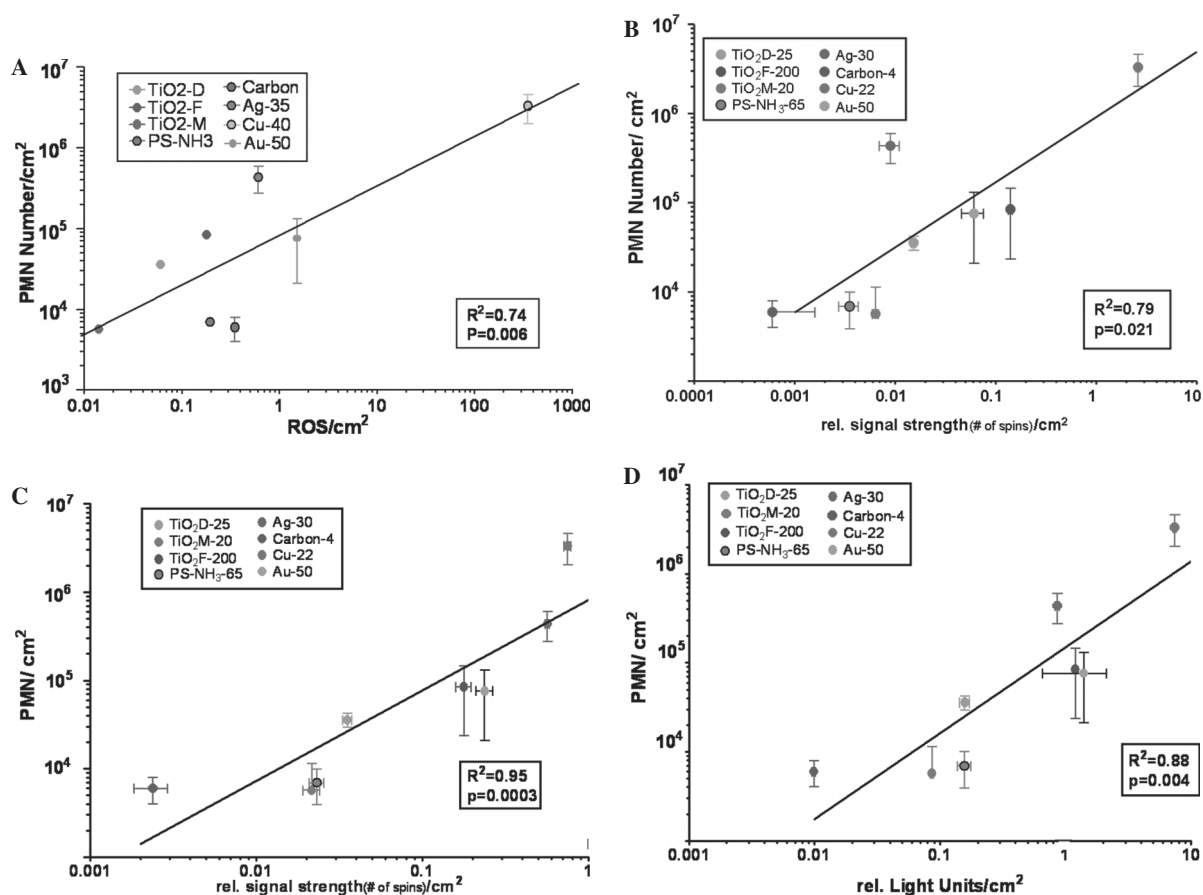
FIGURE 3. Correlations between *in vivo* inflammatory response (number of PMN) and responses observed in cell-free and cellular assays. A box contains the results of correlation analysis with the particle surface area based response-metric (response/cm^2); the R^2 of the Spearman correlation and the significance (p) of the linear fit model. **A**: Cell-free (DCFH oxidation) ROS activity/cm^2 *vs. in vivo* PMN response/cm^2. **B**: Cell-free ESR (DMPO spin trapping) activity/cm^2 *vs. in vivo* PMN response/cm^2. C: Alveolar macrophage ESR (DMPO spin trapping) activity/cm^2 *vs. in vivo* PMN response/cm^2. D: A549 Luc-1 cell luciferase response/cm^2 *vs. in vivo* PMN response/cm^2.

background corrected responses of each assay (Figures 1 and 2) were divided by the total particle surface area utilized to generate the response, resulting in a response per unit surface area as the chemical or biological response metric. Figure 3, A–D, shows the correlations of these responses per unit surface area between the *in vivo* (ordinate) and the other (abscissa) assays based on a linear fit model. These analyses of the calculated correlations and linear fits are reported in Table 3. A good correlation is apparent for all assays and the correlations are significant.

DISCUSSION

In the present study, results of several cell-free and cell-based assays were used to

TABLE 3. Squared Correlations (R^2) and Significance of Linear Models for Comparing Results of Assays Not *In Vivo* With *In Vivo* Assays of Nanoparticle Activity (Log-Transformed Data) Based on NP Surface-Normalized Response Metric

In vivo versus	Spearman correlation, R^2	Significance
Cell-free ROS	0.74	$p = .0064$
Cell-free ESR	0.79	$p = .0208$
ESR with AM	0.95	$p = .0003$
In vitro luciferase	0.88	$p = .0039$

compare the activity of eight different NP in relation to their acute *in vivo* inflammation-generating potency. When the responses were expressed per unit particle surface area, reliable correlations between the *in vivo* and non-*in vivo* results were found, indicating the

usefulness of our proposed concept for predicting *in vivo* responses based on simple *in vitro* assays (Table 3). The two cell-free assays had the lowest correlation coefficients, yet with significance for the linear model, they are reasonably reliable predictors of the acute effects of NP that are observed *in vivo*. ESR was only able to detect the hydroxyl radical, yet the addition of H_2O_2 promotes the formation of this radical from other reactive species. The advantages of the DCF-ROS assay are that the indicator dye has broad oxidant detection compared to others (Luminol, Amplex red, aminophenyl fluorescein, hydroxyphenyl fluorescein, dihydrocalcein-acetomethyl ester, hydroethidine) and that it is simple, gives quick results, and may reasonably predict the ranking of nanomaterials in terms of *in vivo* responses, in particular for identifying highly reactive NP. In the cell-free ESR assay, the result for the Au NP did not agree with the *in vivo* response. However, in the presence of AM, the ESR assay produced results that showed the greatest correlation with the *in vivo* results. The substantial activity of silver NP in this assay with AM, but not without, (Figure 1, b and c) may be due to phagocytosis of Au NP by AM and slow dissolution in the acidic environment of the phagolysosome, which resulted in a greater bioavailability of Au and activation of AM. Obviously the mechanism underrlying this effect requires further investigation. Similarly, the *in vitro* cell assay also showed a reliable correlation with *in vivo* data. It appears, therefore, that assays for predicting *in vivo* responses relative to reference or benchmark particles need to include a cellular component.

For the *in vitro* luciferase investigations, it should be noted that the model system was chosen for its advantages as a screening tool. The A549 Luc1 cells are human lung adenocarcinoma type II-like that have been engineered to produce luciferase under an interleukin (IL)-8 promoter (Singal & Finkelstein, 2005). Increases in luciferase activity correspond to a rise in IL-8 transcription, a chemotactic factor. The more benign particles produced a minimal response in contrast to the more reactive Cu particles, which stimu-lated the cells. This stimulation suggests IL-8 chemokine production, which would result in neutrophil recruitment, an endpoint of acute toxicity that was quantitated in the *in vivo* assay as indicating an oxidative stress response. The production and secretion of IL-8 increase upon activation of nuclear factor (NF)-κB, a transcription factor that is upregulated in the presence of ROS (Chapple 1997; Vlahopoulos et al., 1999; McNeilly et al., 2004; Nam et al., 2004; Ndengele et al., 2005; Auger et al., 2006; Rael et al., 2007; Brown et al., 2007). Consequently, increases in luciferase activity may be correlated to a rise in IL-8 and subsequent neutrophil recruitment.

As useful as the A549 Luc1 cell line is in determining activity and potential toxicity of NP, one could question whether it is the ideal cell line to use for assessing NP toxicity. Although it may represent a pulmonary alveolar type II-like cell, type II cells represent only approximately 5% of the total alveolar surface and therefore may not representative of the primary target of inhaled particulates. Instead, one could argue that a pulmonary alveolar type I-like cell line—type I cells represent approximately 95% of the alveolar surface—should be used for more relevant *in vitro* assays of pulmonary toxicity resulting from nanoparticle exposure since they—and AM as used in the ESR assay—represent primary targets. However, our results indicate that the A549 Luc1 cell assay indeed showed reliable predictive power for acute *in vivo* activity. This cell line may, therefore, be well suited for use in a high-throughput assay.

There is some variance between the results of the two cellular assays, but correlations for both are significant, indicating that the *in vitro* approach can satisfactorily approximate the *in vivo* activity of the different NP. As a point of comparison, when the values are instead normalized per unit mass (µg), the squared correlation coefficient for the luciferase experiment becomes .65 with $p = .0157$. The correlation is still significant; however, this is largely driven by the response to Cu. In general, therefore, data suggest that normalizing responses per unit surface area is preferable as the biological

response metric. This suggestion is also supported by the fact that widely differing specific densities of NPs (e.g., gold vs. PS) renders normalizing responses per unit mass more variable: Gold and PS NP of the same size have the same surface area, but about a 20-fold difference in mass. In general, as suggested repeatedly, surface properties [e.g., charge, reactive groups, defects (Jiang et al., 2008)] appear to be a better dosemetric than mass (Donaldson et al., 2002; Nel et al., 2006; Oberdorster et al., 2005b).

Based on preliminary studies with Cu NP, it was predicted that they would be highly reactive in the assays; therefore, the 40-nm Cu NP was defined as the high benchmark nanoparticle. It was also predicted that TiO_2 would possess low or no activity based on its historical classification as a particle of low toxicity (Ferin, 1971); the 25-nm TiO_2 (P-25, Degussa) was used as the low-activity benchmark nanoparticle. In the cell-free DCF assay, the titanium dioxides produced a minimal response at low dose; however, there was some activity at high doses, making it possible to delineate the activities of the three different TiO_2 NP tested, in particular when activity was expressed per unit dose (surface area). Results of all assays suggest that different TiO_2 samples possess different potencies, which is consistent with our recent results showing different intrinsic ROS-generating potential for TiO_2 particles of different crystal phases (Jiang et al., 2008). Nevertheless, all of the TiO_2 NP are at the low end of the toxicity scale.

Data suggest that a surface area normalized chemical or biological response metric represents a more appropriate NP characteristic for comparison among the different assays than using observed direct assay responses. Normalization of responses per unit surface area can provide a reliable estimate of a NP surface-area-specific activity even if only one dose level is tested, as was done in the present study in all except the DCF-ROS assay. As was pointed out in the introduction, though, this response-metric concept needs to be ideally based on dose-response data covering a wide range of doses so that the steepest part of a dose-response relationship can be identified.

This is considered as a proof-of-principle study designed to introduce the concept of a dose-normalized response metric, which needs to be validated with a more comprehensive data set. Han et al. (2009) recently described an approach to calculate the steepest slope of a dose-response curve mathematically in order to derive the maximum response per unit dose. Alternatively, a more simplistic approach for estimating the value of the steepest slope is illustrated in Figure 4. It is simply defined as the ratio of the difference between two adjacent doses and their responses, provided these doses are in the steepest (linear) portion of the dose-response curve:

$\dfrac{Y_{i+1} - Y_i}{X_{i+1} - X_i}$ is the response per unit dose and

approximates the true value of the steepest slope quite well. This part of the dose-response curve reflects the maximum response per unit dose and is mathematically the maximum of the first derivative. It may be considered as the transition between adaptive (lower doses) and toxic (higher doses) responses. For correlating the outcomes of *in vivo* and *in vitro* assays it is suggested to select the dose and associated response, i.e., response per unit dose, at this transition point of the dose-response relationships. In contrast, using just the highest response, y_n, as measured to represent the toxicological activity in an *in vitro* or *in vivo* assay, is not
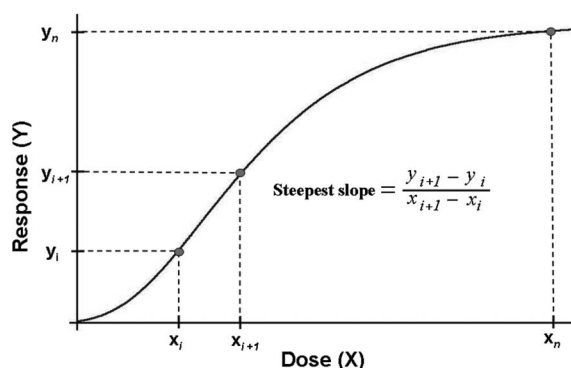
FIGURE 4. Determining the steepest slope as a measure of the response-metric (greatest response per unit dose) from *in vitro* and *in vivo* dose-response curves. The response-metric based on particle surface area as the dose-metric is a more appropriate measure to determine *in vitro/in vivo* correlations than using the highest observed response (y_n) elicited by an unrealistic high dose x_n.

meaningful because the high dose, x_n, is usually not relevant for real-life *in vivo* conditions and will not serve as a meaningful predictor for *in vivo* effects under realistic exposure scenarios.

A recent study by Sayes et al. (2007) provided an opportunity for evaluating our response-metric concept. In that study, five well-characterized different types of nano- and micrometer-sized particles (carbonyl iron, crystalline silica, amorphous silica, nano-sized zinc oxide, and fine-sized zinc oxide) were examined in a well-designed broad-range dose-response design by measuring diverse endpoints of toxicity in three cellular *in vitro* assays using rat AM, rat lung epithelial cells, and co-cultures of these two cell types. Six dose levels, each separated by one order of magnitude, were used in the *in vitro* studies, resulting in well-defined dose-response curves that were determined at 4, 24, and 48 h post dosing. Sayes et al. (2007) compared the *in vitro* results to the pulmonary inflammatory response induced at 24 h and up to 3 mo after intratracheal instillations of the particles in rats and concluded that there was poor correlation between *in vitro* and *in vivo* effects. Indeed, the rankings of particle toxicity did not agree reliably among the assays when comparing the measured highest responses induced by high doses.

In order to test the proposed concept of evaluating correlations between *in vitro* and *in vivo* effects of NPs, the responses reported by Sayes et al. (2007) were expressed as responses per unit particle dose. The responses observed were selected at 24 h because this time point was the only one with results for *in vivo* and all *in vitro* studies. The particles used in their study had been well characterized physicochemically, including the specific surface area. Thus, the particle mass dose-response data were converted to particle surface area dose-response curves, such that one could derive the greatest response per unit particle surface area (steepest slope of dose-response relationship) as described in Figure 4.

Figure 5 shows the results of the steepest slope calculation for two examples of *in vitro/in vivo* correlations from the Sayes *et al.* (2007) study. The first one compares the *in vivo* 24-h pulmonary inflammatory response in rats with the *in vitro* MIP-2 induction by rat AM cultures dosed with the particles (Figure 5, A and B); the second example compares the *in vivo* response with the *in vitro* LDH release in a cell co-culture system (rat AM plus L2 rat lung epithelial cells, Figure 5, C and D). Figures 5A and 5C show the *in vitro/in vivo* correlations when using the originally measured highest responses (equivalent to y_n in Figure 4), whereas Figures 5B and 5D show the results of using instead the highest response per unit particle surface area (steepest slope values). It is apparent that the correlations in Figures 5A and 5C are poor, as was already pointed out by Sayes et al. (2007); in contrast, significant correlations between *in vivo* and *in vitro* results are presented in Figures 5B and 5D. This supports the conclusion from the results of our study that responses observed *in vitro* may well predict *in vivo* responses when using the concept of a surface-area-normalized chemical or biological response metric.

There are obvious limitations to our study. For one, only a limited number of particles were tested in the comparative *in vitro* and *in vivo* assays. Furthermore, although *in vitro* assays can provide valuable mechanistic information, they will only determine acute toxicity and toxicity rankings; they do not, however, provide information about chronic toxicity. Thus, they are useful for the first steps of the four-step risk assessment process, i.e., NP hazard identification and hazard characterization (NRC 1983). Similarly, *in vivo* studies using intratracheal instillations (high dose rate, like *in vitro* studies) do not provide information beyond hazard identification and characterization. Our suggested approach is to obtain information from assays not *in vivo* that have predictive power for *in vivo* responses, which will help to establish a screening strategy that is simple and applicable to a broad range of nanomaterials.

The suggested concept of a NP surface-area-based response metric derived from dose-response relationships could also be considered as a classification/characterization scheme of NP that is based on their chemical (cell-free) and biological/toxicological activity per unit NP surface area (hazard scale) as shown in Table 4. A concept of establishing a "hazard
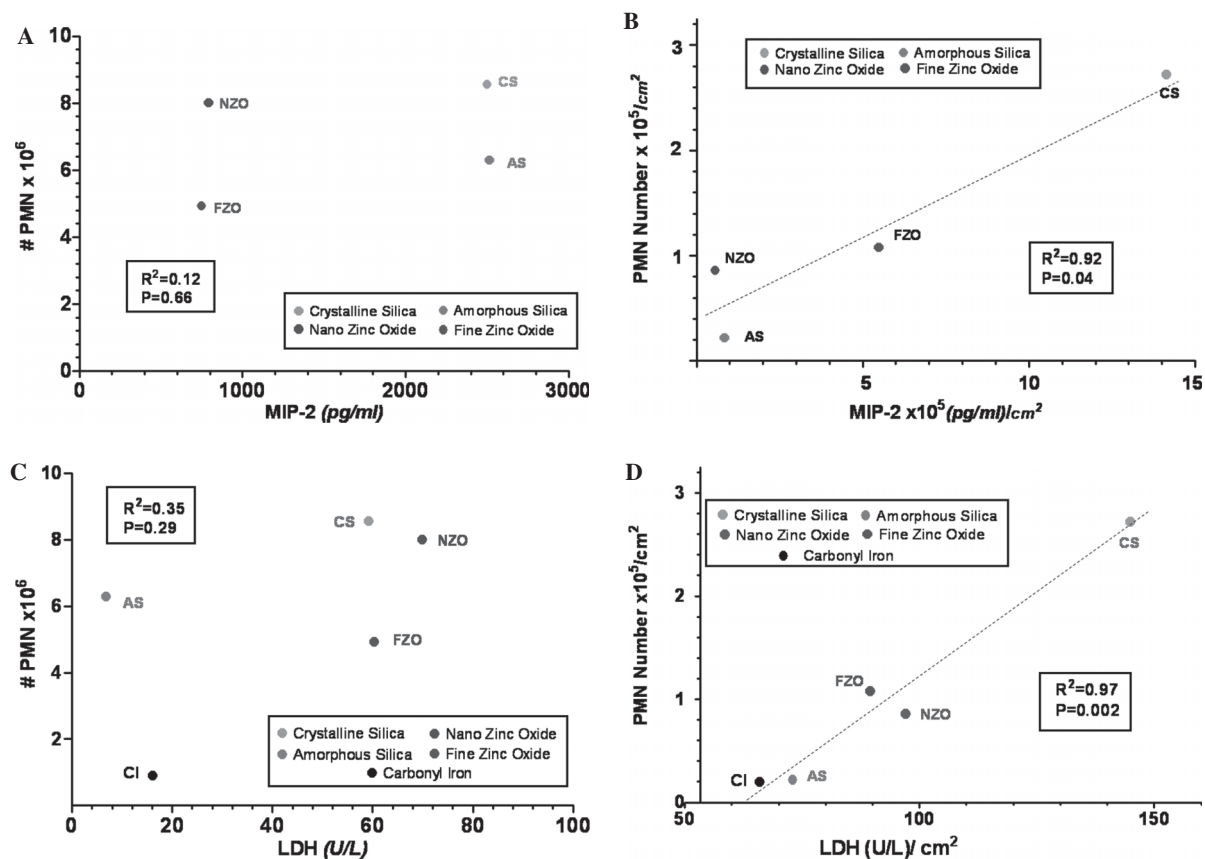
FIGURE 5. Re-analysis of *in vivo/in vitro* correlations of responses of different particles based on dose-relationships observed at 24 hrs. following *in vitro* dosing of lung cells and *in vitro* intratracheal instillations of rats, reported by Sayes *et al*. (2007). For the re-analysis of the data the *in vivo* and *in vitro* responses were either compared based on their highest values as directly determined in the assays (Figs. 5A, C) or they were based on the highest response per unit particle surface area (concept of biological response-metric) calculated from the steepest part of the *in vitro* and *in vivo* dose-response relationships (Figs. 5B;D). Associated Spearman correlations and p-values for significance of linear fit show that expressing *in vitro* data as surface area based response-metrics (derived from steepest slope of dose-response data) has a good predictive power for *in vivo* responses. **A**: *In vivo* (number of PMNs in rat lung lavage) *vs. in vitro* (rat alveolar macrophage induction of MIP-2) correlation, using the highest measured response elicited with high doses of the different particles. **B**: *In vivo* (number of PMNs/cm^2 in rat lung lavage) *vs. in vitro* (rat alveolar macrophage induction of MIP-2/cm^2) correlation, using the highest response per unit particle surface area. *(Note: crystalline silica and amorphous silica are clearly separated in 5B, but not in 5A)*. **C**: *In vivo* (number of PMNs in rat lung lavage) *vs. in vitro* (release of LDH in rat alveolar macrophage + rat type 2 cell-line co-culture) correlation, using the highest measured response elicited with high doses of the different particles. **D**: *In vivo* (number of PMNs/cm^2 in rat lung lavage) *vs. in vitro* (release of LDH/cm^2 in rat alveolar macrophage + rat type 2 cell-line co-culture) correlation, using the highest response per unit particle surface area.

TABLE 4. Example of a Hazard Scale for NP, Based on *In Vitro/In Vivo* Activity per Unit of NP Surface Area

NP type	Hazard category
Carbon black; TiO$_2$ (crystalline state and size dependent)	Very low
TiO$_2$; PS+, Au	Low
Ag	High
Cu	Very high

scale" for NPs may be more meaningful for toxicology and the risk assessment process than classification schemes that classify NP by metals, metal oxides, or polymers. Such activity-based categories of NP may even differentiate among different sizes of NP of the same physicochemical makeup, as shown in our recent study with different sizes of anatase TiO$_2$ (Jiang et al., 2008): Per unit surface area, TiO$_2$ NP approximately 50–200 nm showed a greater activity than TiO$_2$ NP approximately 3–10 nm.

Data indicate that NP-induced acute inflammatory *in vivo* responses relative to benchmark NP may be predicted with simple *in vitro* and cell-free assays, provided that appropriate dose metrics and response metrics are considered. However, important questions about predicting chronic *in vivo* effects are not answered by these simple tests. Particularly useful could be cell-free assays such as DCF oxidation to serve as an initial screening tool to assess a hazard potential of new nanomaterials. More studies need to be completed with the goal to optimize and validate screening assays for predicting short- and long-term NP toxicity so as to avoid more complex, expensive, and ethically objectionable animal studies.

REFERENCES

Auger, F., Gendron, M. C., Chamot, C., Marano, F., and Dazy, A. C. 2006. Responses of well-differentiated nasal epithelial cells exposed to particles: Role of the epithelium in airway inflammation. *Toxicol. Appl. Pharmacol.* 215:285–294.

Balbus, J. M., Maynard, A. D., Colvin, V. L., Castranova, V., Daston, G. P., Denison, R. A., Dreher, K. L., Goering, P. L., Goldberg, A. M., Kulinowski, K. M., Monteiro-Riviere, N. A., Oberdorster, G., Omenn, G. S., Pinkerton, K. E., Ramos, K. S., Rest, K. M., Sass, J. B., Silbergeld, E. K., and Wong, B. A. 2007. Meeting report: Hazard assessment for nanoparticles— Report from an interdisciplinary workshop. *Environ. Health Perspect.* 115:1654–1659.

Barrett, E. G., Johnston, C., Oberdorster, G., and Finkelstein, J. N. 1999. Silica binds serum proteins resulting in a shift of the dose-response for silica-induced chemokine expression in an alveolar type II cell line. *Toxicol. Appl. Pharmacol.* 161:111–122.

Borm, P. J., Robbins, D., Haubold, S., Kuhlbusch, T., Fissan, H., Donaldson, K., Schins, R., Stone, V., Kreyling, W., Lademann, J., Krutmann, J., Warheit, D., and Oberdorster, E. 2006. The potential risks of nanomaterials: A review carried out for ECETOC. *Particl Fibre Toxicol.* 3:11.

Brown, D. M., Hutchison, L., Donaldson, K., MacKenzie, S. J., Dick, C. A., and Stone, V. 2007. The effect of oxidative stress on macrophages and lung epithelial cells: the role of phosphodiesterases 1 and 4. *Toxicol. Lett.* 168:1–6.

Brown, D. M., Wilson, M. R., MacNee, W., Stone, V., and Donaldson, K. 2001. Size-dependent proinflammatory effects of ultrafine polystyrene particles: A role for surface area and oxidative stress in the enhanced activity of ultrafines. *Toxicol. Appl. Pharmacol.* 175:191–199.

Castranova, V., Jones, T., Barger, M. W., Afshari, A., and Frazer, D. G. 1990. Pulmonary responses of guinea pigs to consecutive exposures to cotton dust. *Proceedings 14th Cotton Dust Research Conference*, Memphis, TN.

Cathcart, R., Schwiers, E., and Ames, B. N. 1983. Detection of picomole levels of hydroperoxides using a fluorescent dichlorofluorescein assay. *Anal. Biochem.* 134: 111–116.

Chapple, I. L. 1997. Reactive oxygen species and antioxidants in inflammatory diseases. *J. Clin. Periodontol.* 24:287–296.

Craig, L., Brook, J. R., Chiotti, Q., Croes, B., Gower, S., Hedley, A., Krewski, D., Krupnick.A., krzyzanowski, M., Moran, M. D., Pennell, W., Samet, J. M., Schneideer, J., Shortreed, J., and Williams, M. 2008. Air pollution and public health: A guidance document for risk managers. *J. Toxicol. Environ. Health A* 71:588–698.

Dick, C. A., Brown, D. M., Donaldson, K., and Stone, V. 2003. The role of free radicals in the toxic and inflammatory effects of four different ultrafine particle types. I*nhal. Toxicol.* 15:39–52.

DiMatteo, M., Antonini, J. M., Van Dyke, K., and Reasor, M. J. 1996. Characteristics of the acute phase pulmonary response to silica in rats. *J. Toxicol. Environ. Health* 47:93–108.

Donaldson, K., Brown, D.,Clouter, A.,Duffin, R.,MacNee, W.,Renwick, L., Tran, L., and Stone, V. 2002. The pulmonary toxicology of ultrafine particles. *J. Aerosol Med.* 15:213–220.

Environmental Defense. 2007. *Environmental Defense's activities on nanotechnology*. Environmental Defense, accessed September 25, 2007, www.nanocafes.org/nanoresources/reports_articles.

Ferin, J. 1971. Papain-induced emphysema and the elimination of TiO2 particulates from the lungs. *Am. Ind. Hyg. Assoc. J.* 32:157–162.

Han, X., Finkelstein, J. N., Elder, A., Biswas, P., Jiang, J., and Oberdorster, G. 2009. Dose and response metrics in assessing *in vitro* and *in vivo* nanoparticle toxicity. *Toxicologist* 108: (No.1), pg. 410, Abstract No. 174.

Ibald-Mulli, A., Wichmann, H. E., Kreyling, W., and Peters, A. 2002. Epidemiological evidence on health effects of ultrafine particles. *J. Aerosol Med.* 15:189–201.

Jiang, J., Oberdörster, G., Elder, A., Gelein, R., Mercer, P., and Biswas, p. 2008 Does nanoparticle activity depend upon size and crystal phase? *Nanotoxicology* 2:33–42.

Leonard, S. S., Harris, G. K., and Shi, X. 2004. Metal-induced oxidative stress and signal transduction. *Free Radical Biol. Med.* 37:1921–1942.

Masaki, H., and Sakurai, H. 1997. Increased generation of hydrogen peroxide possibly from mitochondrial respiratory chain after UVB irradiation of murine fibroblasts. *J. Dermatol. Sci.* 14:207–216.

Maynard, A. D. 2007. Nanotechnology: The next big thing, or much ado about nothing? *Ann. Occup. Hyg.* 51:1–12.

Maynard, A. D., Aitken, R. J., Butz, T., Colvin, V., Donaldson, K., Oberdorster, G., Philbert, M. A., Ryan, J., Seaton, A., Stone, V., Tinkle, S. S., Tran, L., Walker, N. J., and Warheit, D. B. 2006. Safe handling of nanotechnology. *Nature* 444:267–269.

McNeilly, J. D., Heal, M. R., Beverland, I. J., Howe, A., Gibson, M. D., Hibbs, L. R., MacNee, W., and Donaldson, K. 2004. Soluble transition metals cause the pro-inflammatory effects of welding fumes *in vitro*. *Toxicol. Appl. Pharmacol.* 196: 95–107.

Nam, H. Y., Choi, B. H., Lee, J. Y., Lee, S. G., Kim, Y. H., Lee, K. H., Yoon, H. K., Song, J. S., Kim, H. J., and Lim, Y. 2004. The role of nitric oxide in the particulate matter (PM2.5)-induced NFkappaB activation in lung epithelial cells. *Toxicol. Lett.* 148 :95–102.

National Research Council. 1983. *Risk assessment in the federal government: Managing the process*. Washington, DC: National Academy Press.

Ndengele, M. M., Muscoli, C., Wang, Z. Q., Doyle, T. M., Matuschak, G. M., and Salvemini, D. 2005. Superoxide potentiates NF-kappaB activation and modulates endotoxin-induced cytokine production in alveolar macrophages. *Shock* 23:186–193.

Nel, A., Xia, T., Madler, L., and Li, N. 2006. Toxic potential of materials at the nanolevel. *Science* 311:622–627.

Oberdorster, G., Ferin, J., and Lehnert, B. E. 1994. Correlation between particle size, *in vivo* particle persistence, and lung injury. *Environ. Health Perspect* 102(suppl. 5): 173–179.

Oberdorster, G., Maynard, A., Donaldson, K., Castranova, V., Fitzpatrick, J., Ausman, K., Carter, J., Karn, B., Kreyling, W., Lai, D., Olin, S., Monteiro-Riviere, N.,Warheit, D., and Yang, H. 2005a. Principles for characterizing the potential human health effects from exposure to nanomaterials: elements of a screening strategy. *Particle Fibre Toxicol.* 2:8.

Oberdorster, G., Oberdorster, E., and Oberdorster, J. 2005b. Nanotoxicology: An emerging discipline evolving from studies of ultrafine particles. *Environ. Health Perspect* 113 :823–839.

Porter, D. W., Barger, M., Robinson, V. A., Leonard, S. S., Landsittel, D., and Castranova, V. 2002. Comparison of low doses of aged and freshly fractured silica on pulmonary inflammation and damage in the rat. *Toxicology* 175 :63–71.

Rael, L. T., Rao, N. K., Thomas, G. W., Bar-Or, R., Curtis, C. G., and Bar-Or, D. 2007. Combined cupric- and cuprous-binding peptides are effective in preventing IL-8 release from endothelial cells and redox reactions. *Biochem. Biophys. Res. Commun.* 357:543–548.

Sayes, C. M., Reed, K. L., and Warheit, D. B. 2007. Assessing toxicity of fine and nanopar-

ticles: Comparing *in vitro* measurements to *in vivo* pulmonary toxicity profiles. *Toxicol. Sci.* 97:163–180.

Singal, M., and Finkelstein, J. N. 2005. Use of indicator cell lines for determining inflammatory gene changes and screening the inflammatory potential of particulate and non-particulate stimuli. *Inhal. Toxicol.* 17: 415–425.

The Royal Society and the Royal Academy of Engineering (UK). 2004. *Nanoscience and nanotechnologies: Opportunities and uncertainties*. www.royalsoc.ac.uk.

U.S. Environmental Protection Agency. 2004. *Air quality criteria for particulate matter*. October. Washington, DC: U.S. Environmental Protection Agency.

US Environmental Protection Agency. 2007. *Nanotechnology white paper*. Washington, DC: Science Policy Council, U.S. Environmental Protection Agency.

Utell, M. J., and Frampton, M. W. 2000. Acute health effects of ambient air pollution: The ultrafine particle hypothesis. *J. Aerosol Med.* 13:355–359.

Venkatachari, P., Hopke, P., Grover, B., and Eatough, D. 2005. Measurement of particle-bound reactive oxygen species in Rubidoux aerosols. *J. Atmos. Chem.* 50:49–58.

Vlahopoulos, S., Boldogh, I., Casola, A., and Brasier, A. R. 1999. Nuclear factor-kappaB-dependent induction of interleukin-8 gene expression by tumor necrosis factor alpha: Evidence for an antioxidant sensitive activating pathway distinct from nuclear translocation. *Blood* 94:1878–1889.

von Klot, S., Peters, A., Aalto, P., Bellander, T., Berglind, N., D'Ippoliti, D., Elosua, R., Hormann, A., Kulmala, M., Lanki, T., Lowel, H., Pekkanen, J., Picciotto, S., Sunyer, J., and Forastiere, F. 2005. Ambient air pollution is associated with increased risk of hospital cardiac readmissions of myocardial infarction survivors in five European cities. *Circulation* 112:3073–3079.